Hybrid diffuse optical techniques for continuous hemodynamic measurement in gastrocnemius during plantar flexion exercise

Brad Henry
Mingjun Zhao
Yu Shang
Timothy Uhl
D. Travis Thomas
Eleftherios S. Xenos
Sibu P. Saha
Guoqiang Yu

Hybrid diffuse optical techniques for continuous hemodynamic measurement in gastrocnemius during plantar flexion exercise

Brad Henry,[a,†] Mingjun Zhao,[a,†] Yu Shang,[a] Timothy Uhl,[b] D. Travis Thomas,[c] Eleftherios S. Xenos,[d] Sibu P. Saha,[d] and Guoqiang Yu[a,*]
[a]University of Kentucky, College of Engineering, Department of Biomedical Engineering, 143 Graham Avenue, Lexington, Kentucky 40506-0108, United States
[b]University of Kentucky, College of Health Sciences, Department of Rehabilitation Science, 900 S Limestone Street, Lexington, Kentucky 40536-0200, United States
[c]University of Kentucky, College of Health Sciences, Department of Clinical Sciences, 900 S Limestone Street, Lexington, Kentucky 40536-0200, United States
[d]University of Kentucky, College of Medicine, Department of Surgery, 900 S Limestone Street, Lexington, Kentucky 40536-0200, United States

Abstract. Occlusion calibrations and gating techniques have been recently applied by our laboratory for continuous and absolute diffuse optical measurements of forearm muscle hemodynamics during handgrip exercises. The translation of these techniques from the forearm to the lower limb is the goal of this study as various diseases preferentially affect muscles in the lower extremity. This study adapted a hybrid near-infrared spectroscopy and diffuse correlation spectroscopy system with a gating algorithm to continuously quantify hemodynamic responses of medial gastrocnemius during plantar flexion exercises in 10 healthy subjects. The outcomes from optical measurement include oxy-, deoxy-, and total hemoglobin concentrations, blood oxygen saturation, and relative changes in blood flow (rBF) and oxygen consumption rate ($r\dot{V}O_2$). We calibrated rBF and $r\dot{V}O_2$ profiles with absolute baseline values of BF and $\dot{V}O_2$ obtained by venous and arterial occlusions, respectively. Results from this investigation were comparable to values from similar studies. Additionally, significant correlation was observed between resting local muscle BF measured by the optical technique and whole limb BF measured concurrently by a strain gauge venous plethysmography. The extensive hemodynamic and metabolic profiles during exercise will allow for future comparison studies to investigate the diagnostic value of hybrid technologies in muscles affected by disease. © *2015 Society of Photo-Optical Instrumentation Engineers (SPIE)* [DOI: 10.1117/1.JBO.20.12.125006]

Keywords: near-infrared spectroscopy; diffuse correlation spectroscopy; blood flow; blood oxygenation; oxygen consumption rate; gastrocnemius; plantar flexion exercise.

Paper 150477RR received Jul. 15, 2015; accepted for publication Nov. 20, 2015; published online Dec. 23, 2015.

1 Introduction

Observation of skeletal muscle hemodynamics has long been viewed as a critical part of understanding how the tissue adapts to metabolic stresses that are applied during exercise and disease states.[1–9] Understanding how the healthy muscle reacts to different perturbations allows researchers and clinicians to evaluate how disease states affect the muscle's performance. Given the complexity of the operation of muscle tissue and the dynamically regulated interplay of local versus global controls of blood perfusion in response to the tissue demand for oxygen, mechanical effects, and aggregation of feedback metabolites, it is no wonder that muscle physiology and diseases thereof remain a highly active field of study.[5,10–17]

Our particular interest is the mechanism of local muscle action and the specific pathology of peripheral arterial disease (PAD). PAD is emphasized in muscle research because it is associated with a rather high morbidity and has a distinctly detrimental effect on the patient's health and quality of life.[5,18–20] Since diseases such as PAD induce tissue-level effects related to the skeletal muscle hemodynamics, it is most efficient to study these diseases by the examination of local muscle hemodynamics. Invasive methods of monitoring local muscle hemodynamics all suffer the same weakness in that they are clinically more dangerous due to increasing the risk of infection, inducing some degree of stress in the patient, and being inapplicable for continuous monitoring during dynamic protocols.[21,22] Functional magnetic resonance imaging (MRI) and positron emission tomography (PET) stand out as effective methods for assessing tissue blood flow (BF) and oxygenation as well as having the additional capability of measuring crucial metabolic parameters such as phosphate metabolites. The weakness of these two technologies is their expense to employ. PET is still reliant on the use of radioactive elements, and both require confinement to measurement tubes and limit the modalities of exercise that may be employed.[21,23–25]

The use of near-infrared (NIR) diffuse optical methods allows continuous, rapid, and noninvasive acquisition of local deep tissue hemodynamics. The optical window of tissue (600 to 950 nm) allows NIR source light to illuminate tissue several centimeters beneath the skin. NIR spectroscopy (NIRS) oximetry is widely accepted to be reliable in the determination of oxy-hemoglobin (HbO_2), deoxy-hemoglobin (Hb), total hemoglobin concentration (THC), and blood oxygen saturation (StO_2) in deep tissues.[8,26–30]

Diffuse correlation spectroscopy (DCS) flowmetry is a more recent application of dynamic NIRS, which has been developed to examine relative blood flow (rBF) changes within deep tissue

---

microvasculature.[6,22,31] DCS operates on the principle that photons injected into biological tissues diffuse and generate time-varying light speckle fluctuations due to the motion of moving scatterers in the tissue (e.g., red blood cells). The light speckle fluctuations can be detected by photon detectors and quantified by calculating the photon electric field autocorrelation function to yield a blood flow index (BFI).[31] This flow index is normalized to an initial period of baseline to produce rBF.[6,9,32] DCS has been validated against multiple techniques, such as Xenon-computed tomography, arterial-spin-labeled MRI, and laser Doppler,[22,25,33] and has proven successful in making rBF measurements of local muscles in the leg and forearm.[6,9,32,34–36] In some of these studies, DCS has been combined with NIRS to form a hybrid DCS/NIRS instrument for making all-optical measurements of both rBF and StO_2, which allows for the derivation of the relative change of oxygen consumption rate ($r\dot{V}O_2$).[6,9,22,34]

Only recently have occlusion calibrations and gating techniques been applied by our laboratory to allow DCS/NIRS hybrid instruments to simultaneously and continuously measure absolute values of BF, blood oxygenation, and oxygen consumption rate ($\dot{V}O_2$) in forearm muscles during handgrip exercises.[9] The translation of these techniques from the arm to the lower limb is the goal of this study as various diseases (such as PAD) affect muscle tissue perfusion and metabolism preferentially in the lower limb. This research then focused on developing calibration and exercise protocols for use in the lower limb that would be comparable to those of literature and, optimally, could be done by both healthy controls and PAD patients. The success in producing consistent and comparable hemodynamic responses in gastrocnemius (calf) muscles would determine if our techniques were sound and would offer a platform to extend measurement to patient populations.

To achieve these goals, we modified our fiber-optic probe originally designed for the forearm muscle measurement and applied a larger source–detector (S-D) distance to probe deeper calf muscles. We bundled multiple detector fibers together for BF measurements and then averaged the detected signals collected from these fibers, which significantly improved the signal-to-noise ratio (SNR) of DCS measurements. Following our previous study in forearm muscles,[9] we applied calibrated diffuse optical measurements and gated exercise protocols to examine absolute values of tissue hemodynamics and metabolism in working calf muscles of the lower limb. In addition, we compared baseline BF in local calf muscles measured by NIRS and whole leg BF measured concurrently by a strain gauge venous plethysmography (SGVP). Concurrent NIRS and SGVP measurements of baseline BF have been previously done in forearms using venous occlusion (VO) protocols,[4,37,38] but not in legs. The dynamic responses of hemodynamic/metabolic parameters to calibrating occlusions, plantar flexion exercise, and postexercise recovery measured by these optical techniques were corroborated by comparing them to responses obtained by other techniques using similar protocols.[5,12,13,18,39] Overall, this study moves the hybrid diffuse optical techniques closer to clinical application in patient populations.

2 Methods

2.1 Subject Characteristics

Ten young, healthy subjects (eight male, two female) volunteered to participate in this study, and all gave their consents via signed institutional review board approved forms. The average age of the subjects was 28 ± 3 years, and average subject strength, determined by maximal voluntary isometric contraction (MVIC),[9] was 93.7 ± 26.5 Nm. The subjects had an average adipose tissue thickness (ATT) of 6.4 ± 1.5 mm (measured by a skinfold caliper), which was well short of the detection depth for NIR photon paths.[6,13,40,41] All subjects had some history of recreational training but were not athletes. The subjects were measured before they had performed any exercises on a given day.

2.2 Experimental Design

Subject muscle hemodynamics were assessed during three different hemodynamic challenges: (1) a series of 50 mm Hg VOs, which were used to calibrate rBF (measured by DCS) to absolute BF, (2) a single 250 mm Hg arterial occlusion (AO), which was used to calibrate $r\dot{V}O_2$ to absolute $\dot{V}O_2$, and (3) a 30% MVIC plantar flexion exercise for 3 min, which was used to examine working muscle hemodynamics and metabolism with the hybrid DCS/NIRS device.

Before exercise, three calibrating VOs were recorded with both DCS/NIRS and SGVP to compare local tissue BF against limb BF. Similarly, an immediate postexercise VO was applied to assess SGVP limb BF for comparison with end-exercise muscle BF measured by DCS. Muscle hemodynamic recovery from exercise was continuously recorded by the hybrid DCS/NIRS for 15 min postexercise. Systemic heart rate (HR) and mean arterial pressure (MAP) were recorded continuously by a finger plethysmograph sensor throughout exercise to examine global cardiovascular responses to exercise.

2.3 Experimental Protocols

Each subject was placed in a supine position with the right foot secured to a dynamometer (Primus, BTE, Hanover, MD) foot plate via adjustable Velcro straps (see Fig. 1). ATT was determined using a skinfold caliper (Lange 85300, Texas). A pillow supported the backs of the knee to allow the subject to relax without placing a hyperextention/enforced extension of the knee. A pressure/occlusion cuff (Zimmer ATS 1000, Indiana) was affixed to the thigh of the right leg. The optical probe was then secured to the medial gastrocnemius by using two strips of cotton surgical tape: one 3×8 in. aligned with the long axis of the limb and the other 3×4 in. long around the circumferential axis. The probe was carefully attached so as to remain in contact with the skin without applying excessive pressure, a condition that may cause hemodynamic variations.[42–44] The optical fibers connected to the probe were then taped to the measurement chair to reduce the effect of their weight on the probe/tissue interface. A strain gauge with loop lengths of 26 to 32 cm (Hokanson E8, Massachusetts) was placed at the proximal end of the optical probe just above the site of greatest circumference. The entirety of the physical setup is exemplified in Fig. 1.

Following attachment of measuring devices, a 3-min baseline period was recorded to ensure hemodynamic stability. After the baseline measurement, three VOs (50 mm Hg tourniquet pressure for 10 s) were performed, each with 1 min between to allow tissue hemodynamics return to rest. Upon completion of the three VOs, tourniquet pressure was increased to fully occlusive levels (~250 mm Hg); a single AO was performed for 3 min. Subject recovery was monitored following the AO for 5 min. After the recovery, MVIC was assessed by instructing the subject to perform three to five maximum effort contractions to
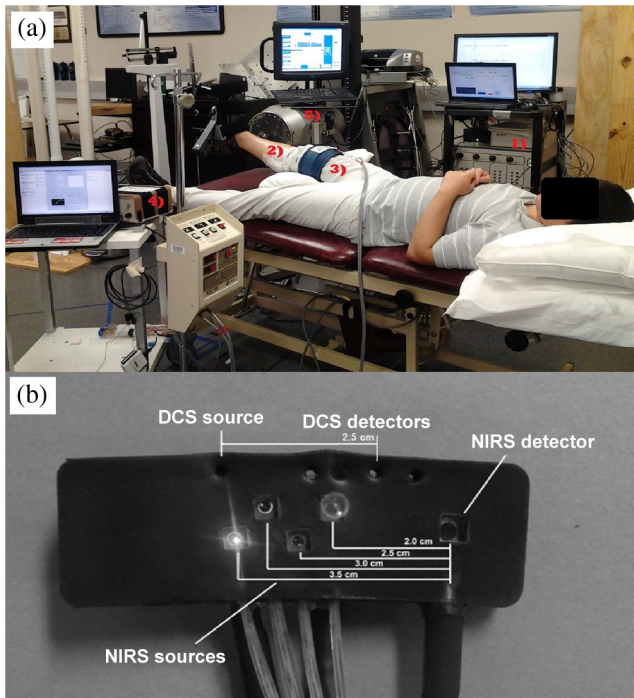
Fig. 1 (a) Experimental setup: (1) diffuse correlation spectroscopy (DCS)/near-infrared spectroscopy (NIRS) hybrid equipment received analog position input from the dynamometer to gate data collection during exercise. (2) Optical probe [depicted uncovered in (b)] sited over medial gastrocnemius at the location of the muscle belly. (3) Occlusion cuff secured above the thigh for inducing venous and arterial occlusions (VO and AO) for calibration. (4) The strain gauge and control computer run independently and concurrently during both calibration and exercise protocols. (5) The dynamometer was used to control exercise workload and frequency via setting 30% maximal voluntary isometric contraction (MVIC) resistance and passive return to rest. A visual metronome was used to regulate subject timing.

generate a force plateau. The average of these forces was set as the final mean MVIC. The difference in exercise strength between subjects (particularly male and female) was normalized by using 30% MVIC exercise load. After MVIC determination, the subject was given a brief instruction/training (approximately five consecutive successful duty cycles) to practice consistent

timing and exercise duty cycles. A single duty cycle consisted of starting from a neutral 90 deg ankle angle, contracting smoothly through 30 deg over a period of 0.5 s, relaxing back to rest for the same, and remaining at rest for 1 s. This rhythm was displayed on the dynamometer monitor via a visual metronome and supplemented by investigator prompting to assist subjects in maintaining the proper contraction/rest sequence.

After training, the subject was then instructed to rest while a finger plethysmograph sensor (Portapres, FMS, The Netherlands) for noninvasive and continuous monitoring of MAP and HR was secured to the right index finger. Calibration data files were saved and data collection settings were adjusted for plantar flexion exercise (~5 min). Subject baseline stability was confirmed by observing 3 min of resting data. Subjects were then cued to begin 3 min of 0.5 Hz, 30% MVIC, full range of plantar flexion motion (15 to 30 deg). Upon signaling the end of exercise, a single VO was immediately performed for assessing SGVP limb BF, followed by a recovery recording for 15 min. Figure 2 diagrams the entire protocol procedure.

2.4 Data Acquisition

We have built a hybrid instrument combining commercial NIRS oximetry (Imagent, ISS, Illinois) and custom-made DCS flowmetry to collect tissue hemodynamic data.[45] NIRS in practice is well documented, so the operation of the particular device used is summarized briefly. The Imagent illuminates tissue with four alternating laser diodes (i.e., 690, 750, 780, and 830 nm, modulated at 110 MHz) at each source position. There are a total of four source positions placed at four different distances (2.0, 2.5, 3.0, and 3.5 cm) away from the single detector along a line axis, as shown in Fig. 1(b). All laser diodes (16 in total) are turned on alternatively in a time-multiplex manner. Frequency-domain spectroscopy analysis at multiple S-D distances (a process denoted as spatially resolved spectroscopy) yields absolute values of tissue absorption coefficient (μ_a), reduced scattering coefficient (μ_s'), and hemoglobin concentrations.[8,27,30] A further step to reduce phase noise from detected light is taken in which the amplitude data from 830 and 690 nm sources are used from the 2.5 cm S-D distance to calculate relative hemoglobin concentrations (via Beer–Lambert law calculation), and these
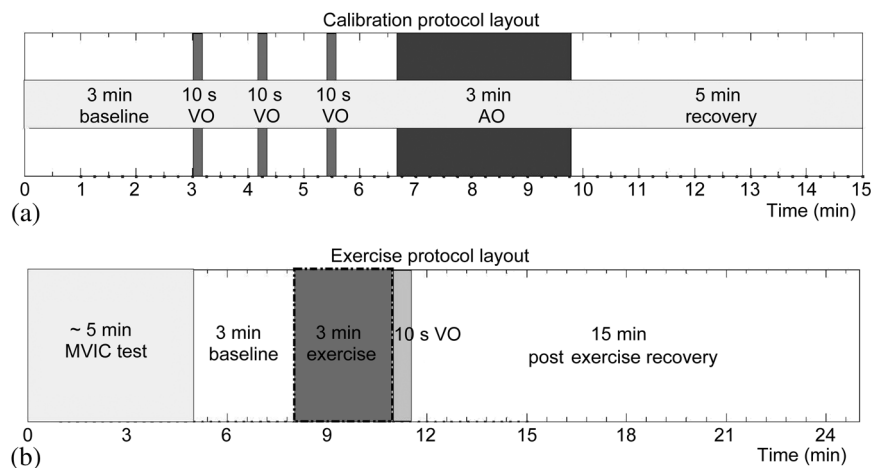
Fig. 2 Protocol layout for (a) venous and arterial calibrations and (b) 30% MVIC plantar flexion exercise. The diagram summarizes the duration and timing for each procedure. The black dotted box signifies the period in which the gating algorithm was active to reduce muscle motion artifacts.

are then calibrated via addition to a baseline of absolute data.[9] This process generates absolute values of [HbO$_2$], [Hb], THC (THC = [Hb] + [HbO$_2$]), and StO$_2$ (StO$_2$ = [HbO$_2$]/THC × 100%).

DCS instrumentation is likewise documented and consists of source light injection from a long coherence laser (785 nm, Crystalaser, Nevada) and detection via four single-mode detector fibers 2.5 cm away. Speckle intensity signals are transmitted to four single photon counting avalanche photon detectors (APDs, PerkinElmer Inc., Canada). The light intensity signals are then input to a multichannel autocorrelator board (Correlator.com, New Jersey) to produce normalized intensity autocorrelation curves (g$_2$), which can then be averaged (improving SNR by a factor of 2) and used to calculate BFI by the use of correlation diffusion theory.[22,31] More specifically, the measured intensity autocorrelation function is related to an electric field autocorrelation function, denoted $G_1(\tau)$, which is modeled as the solution of a correlation diffusion equation for tissues with semi-infinite geometry.[34,46] Decay of the electric field autocorrelation function is dependent on μ_a, μ_s', and a parameterized diffusive flow of dynamic scatterers (i.e., moving red blood cells). This diffusive flow index is described by αD_B, that is, the effective Brownian diffusion coefficient (D_B) multiplied by the ratio of dynamic versus static scatterers (α). This flow index is then normalized to a baseline value collected before physiological changes to produce rBF.

DCS/NIRS measures a mixture of superficial and deep tissues because photons propagate throughout both top layer adipose tissues and deep muscle tissues. Based on photon diffusion theory, light penetration depth depends on tissue optical properties and S-D distance, and it is approximately one half of the S-D distance. This study used relatively large S-D distances (2.5 cm for DCS and 2 to 3.5 cm for NIRS) to collect the data, which allowed light to penetrate thorough the top layer adipose tissues (ATT = 6.4 ± 1.5 mm) to the deep calf muscles.

During baseline calibration measurements, it is necessary to increase the NIRS sample rate to precisely capture rapid changes in hemoglobin concentration during 10-s VO and the early time of AO. A sampling rate of 7 Hz was used for Imagent to collect five data points consecutively. A transistor–transistor logic signal between the Imagent and DCS consoles then deactivated Imagent sources/detectors and activated DCS sources/detectors for a 0.3-s autocorrelation averaging time to collect a single rBF datum. The overall sampling rate was ~1 Hz to produce one data point for DCS and five data points for Imagent. Baseline absolute BF was obtained by fitting the slope of the THC increase measured by Imagent during VO,[18,28,35,40] while baseline absolute V̇O$_2$ was calculated by fitting the slope of the difference between [HbO$_2$] and [Hb] during the first minute of AO.[9,41]

Following baseline calibrations, sampling for the hybrid DCS/Imagent was changed to a one-to-one with 1 Hz overall sampling rate for use in the exercise protocol: 600 ms for DCS correlation plus 300 ms for Imagent sampling. Due to the sensitivity of DCS to muscle fiber motion artifacts, a gating exercise algorithm was used to limit DCS data collection to only the rest periods between muscle contractions, as determined by an analog signal generated by the dynamometer.[9]

The outcomes from the continuous hybrid measurements during exercise included rBF, [HbO$_2$], [Hb], and StO$_2$, which were used to calculate rV̇O$_2$ [rV̇O$_2$ = rBF × (1 − StO$_2$)/(1 − StO$_{2baseline}$). Here, StO$_{2baseline}$ represented the pre-exercise

baseline value of StO$_2$. Finally, the rBF and rV̇O$_2$ data during exercise were calibrated with the absolute baseline BF and absolute baseline V̇O$_2$ obtained through the VO and AO protocols, respectively.

The strain gauge was activated simultaneously with the hybrid optical instruments, electronically calibrated, and run continuously during protocols with data aligned in postprocessing via file time stamps. The sampling rate of SGVP was set at 100 Hz with an average of 50 raw data points for overall data recording at 2 Hz. In addition to local leg hemodynamics, systemic parameters (MAP and HR) were measured using a finger plethysmograph. These measurements concurrently provided local muscle tissue and systemic profiles of response to exercise.

2.5 Data Analysis

Time course data from all subjects were aligned based on the individual marks made at the beginning and end of the exercise for group averaging. To evaluate group mean values at specific time points (i.e., baseline-exercise, end-exercise, 1-min recovery postexercise, end-recovery), average values were selected at the last 2 min of baseline before exercise, last 1 min of exercise, first 1 min of recovery immediately postexercise, and last 2 min end of recovery measurements. Because of the limited sample size ($n = 10$), some of the parameters did not meet normal distribution criteria as determined by Shapiro Wilk tests. To keep the statistic method consistent for all parameters, Friedman's tests were used for all parameters to analyze the effect of time periods. If the effect of time periods was identified to be significant, further analyses using Wilcoxon signed-rank tests were conducted for pairwise comparisons. Linear regressions were performed for the comparison of concurrent SGVP and optical measurements of BF. $p < 0.05$ was considered significant for all statistical results. All statistical analyses were implemented by the statistics toolbox of MATLAB® 2010b (Mathworks Inc., Massachusetts).

3 Results

3.1 Baseline Calibrations

An illustrative subject's hemodynamic profiles during VO and AO calibrations are shown in Fig. 3, with special emphasis on occlusion periods displayed in Fig. 4. VO responses show increased [HbO$_2$] and THC and a slight decrease in rBF for each occlusion with a clear increase in limb volume as measured by the strain gauge. These changes show consistently successful VOs for rBF calibrations. During the AO, rBF dropped to near zero, confirming the complete occlusion of the compartment. An initial increase in THC was observed at the beginning of AO, which was likely due to the delay of occlusion pressure reaching to the thigh cuff. In some subjects, a slight but continuous increase in THC was also observed, indicating limited arterial leakage (see the hemoglobin and strain gauge trends in Fig. 3). This response has been noted in several studies and is representative of the ability of the microvasculature to allow fluid volumes to shunt even under highly claudicant pressures.[9,18]

Individual baseline BF and V̇O$_2$ obtained from the VO and AO calibrations are summarized in Table 1. Baseline BF values measured by optical device and SGVP were found to be positively correlated ($R^2 = 0.51$, $p < 0.05$, Fig. 5).
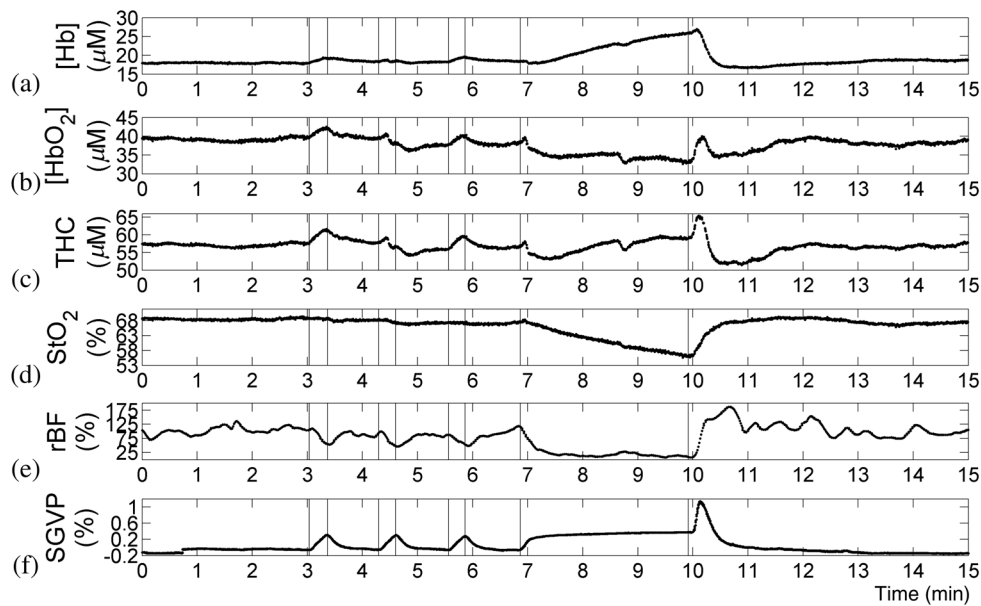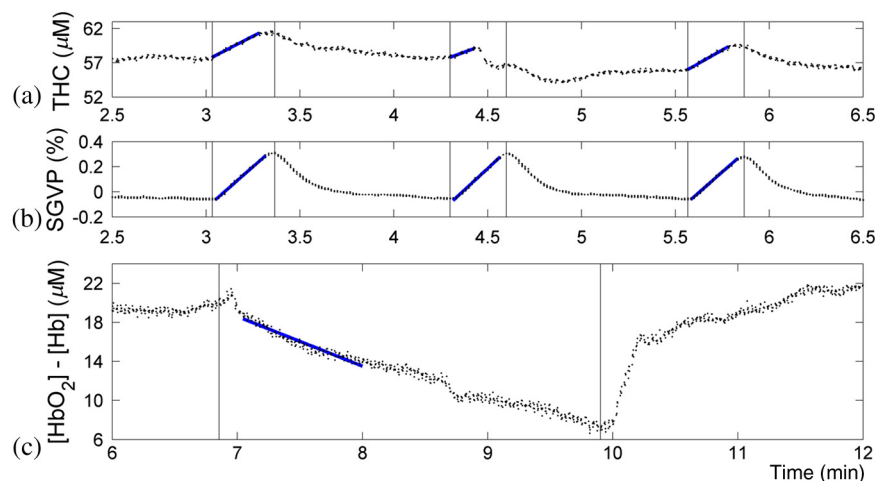
Fig. 3 Illustrative subject (subject 4) hemodynamic and strain gauge data during calibration protocols; descending order (a) to (f): [Hb], [HbO$_2$], total hemoglobin concentration (THC), blood oxygen saturation (StO$_2$), relative changes in blood flow (rBF), and strain gauge venous plethysmography (SGVP). Raw rBF data were filtered with second-order Butterworth low-pass filter (cut-off frequency: 0.033 Hz) to reduce high-frequency noises. Hemodynamic trends indicated successful VO and AO.

3.2 Exercise Responses

The exercise produced consistent dynamic trends, but intrasubject variations existed in most hemodynamic parameters. Group mean hemodynamic profiles are displayed in Fig. 6, with Table 2 numerically summarizing the parameters measured during the baseline-exercise, end-exercise, and recovery periods. Friedman's tests suggested that the effects of time periods were significant for all the parameters measured. Therefore, further analyses using Wilcoxon signed-rank tests were conducted for all parameters.

The initial response to muscle contraction shows obvious divergence in muscle hemodynamics from baseline to exercise status. StO$_2$ and THC decreased rapidly, while rBF and r$\dot{V}O_2$ climbed steeply. Compared to rBF ($216.00 \pm 30.30\%$), r$\dot{V}O_2$ exhibited greater responses to exercise with increases of $324.40 \pm 41.50\%$. End-exercise values of StO$_2$ reached an average of $57.80 \pm 3.10\%$ from the baseline values of $72.70 \pm 1.00\%$. All hemodynamic parameters reached a stable plateau within ~2 min of the exercise. Systemically, both HR and MAP increased very rapidly, which, combined with local


Fig. 4 Zoomed-in view of the illustrative subject (subject 4) calibration occlusion responses. (a) The optical THC slope during VO was used to calculate arterial inflow (baseline BF). A MATLAB® polyfit function was used to determine the slope. (b) The SGVP slope during VO was used to calculate baseline limb BF. Simultaneous time registries indicated both methods to determine BF are sensitive to VO. (c) The hemoglobin concentration change slope ([HbO$_2$] − [Hb]) during AO was used to determine baseline oxygen consumption rate ($\dot{V}O_2$). Optical data showed initial increases as the pressure cuff reached VO pressure and then AO pressure. One-minute AO is sufficient to calculate $\dot{V}O_2$, whereas 3-min AO was used to confirm hyperemic response and verify occlusion integrity.

Table 1 Absolute baseline values of blood flow (BF) and oxygen consumption rate ($\dot{V}O_2$) calibrated by venous occlusion (VO) and arterial occlusion (AO) protocols.

Subject	VO calibrated optical BF (ml/100 ml/min)	VO calibrated strain gauge venous plethysmography (SGVP) BF (ml/100 ml/min)	AO calibrated optical $\dot{V}O_2$ (ml O_2/100 g/min)
1	1.04 ± 0.06	1.18 ± 0.05	0.009
2	1.36 ± 0.11	2.40 ± 0.07	0.127
3	1.33 ± 0.06	1.94 ± 0.15	0.023
4	0.61 ± 0.13	1.29 ± 0.08	0.057
5	0.62 ± 0.16	1.03 ± 0.06	0.030
6	0.35 ± 0.16	0.57 ± 0.09	0.036
7	1.03 ± 0.35	0.46 ± 0.16	0.058
8	0.46 ± 0.01	0.41 ± 0.03	0.027
9	0.95 ± 0.35	1.04 ± 0.10	0.059
10	1.07 ± 0.32	1.01 ± 0.06	0.068
Group mean	0.88 ± 0.35	1.13 ± 0.63	0.049 ± 0.033

BF is shown as the mean $\pm$ standard deviation of the three VO measurements, while $\dot{V}O_2$ is shown as a single measurement only. Group values are presented as means $\pm$ standard errors.
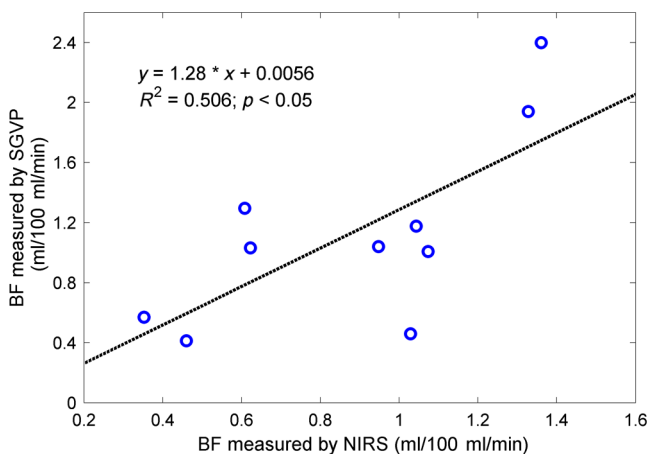
Fig. 5 Linear regression of BF values measured by NIRS and SGVP. A correlation of $R^2 = 0.51$ was obtained, indicating a sound correlation between the two measurements despite high degrees of intrasubject variation. BF measured by SGVP is generally higher than NIRS measurements, as has been noted by many previous studies.

tissue responses, supported our assertion that the exercise was physically demanding.

The correlation between the strain gauge and optical measurements was erased in the face of widely variant measurements of BF between local and limb exercise responses for individuals. Individual responses varied largely within both measurements with 1-min recovery values for local BF and
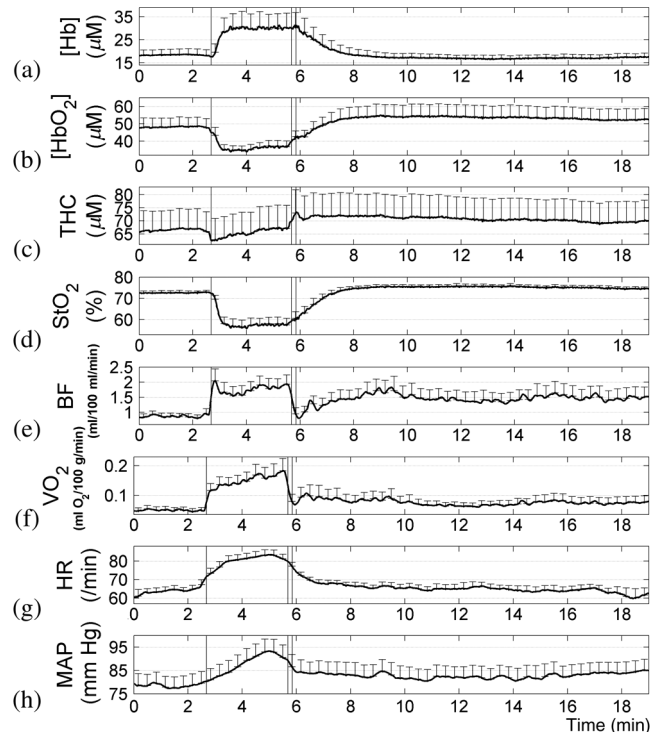
Fig. 6 Group mean ($n = 10$) hemodynamic and metabolic profiles of gastrocnemius muscle during exercise; descending order (a) to (h): [Hb], [HbO$_2$], THC, StO$_2$, BF, $\dot{V}O_2$, heart rate, and mean arterial pressure (MAP). For MAP, subject 1 is excluded because of poor data quality. Group means were calculated after aligning each subject's time series with the beginning and end of the exercise period. BF time series of each subject were filtered with a second-order Butterworth low-pass filter (cut-off frequency: 0.033 Hz) to reduce the high-frequency noises before calculating group mean. The three marks in each panel denote the beginning and end of the exercise, as well as the VO applied immediately after exercise for the SGVP BF calibration. Responses to exercise were rapid and immediately observable from all measurements. BF values immediately after exercise ($5.13 \pm 0.32/100$ ml/min) measured by SGVP (data are not shown in the figure) were much greater than those ($1.05 \pm 0.17/100$ ml/min) measured by DCS.

SGVP limb BF being 1.09 ± 0.19 ml/100 ml/min and 5.13 ± 0.32 ml/100 ml/min, respectively (Fig. 6).

3.3 Postexercise Recovery

The postexercise recovery (Fig. 6 and Table 2) occurred for most measured parameters within the first minute and was stable but incomplete by the second minute following exercise; the trend persisted during subsequent observed recovery periods. However, compared to baseline values, there were significant elevations in r$\dot{V}O_2$ ($158.30 \pm 16.60\%$ versus $100.00 \pm 0.00\%$) and to a lesser extent rBF ($118.80 \pm 8.20\%$ versus $100.00 \pm 0.00\%$) and MAP (84.30 ± 10.00 mm Hg versus 78.50 ± 9.40 mm Hg) during the 1-min recovery period. Comparing end-exercise with 1-min recovery, rBF ($216.00 \pm 30.30\%$ versus $118.80 \pm 8.20\%$) and r$\dot{V}O_2$ ($324.40 \pm 41.50\%$ versus $158.30 \pm 16.60\%$) recovered larger and quicker than StO$_2$ ($57.80 \pm 3.10\%$ versus $64.10 \pm 3.00\%$). HR recovered rapidly and returned at the end-recovery [61.90 ± 3.40 beats per minute (BPM)] to close to its baseline level (64.70 ± 2.10 BPM), indicating a return of cardiac output to baseline levels. Overall, the significant elevations in MAP and local hemodynamic/

Table 2 Group averaged BF, blood oxygen saturation (StO$_2$), oxygen consumption rate ($\dot{V}O_2$), mean arterial pressure (MAP), and heart rate (HR) before, during, and after exercise ($n = 10$).

Hemodynamic parameters	Baseline exercise	End-exercise	1-min recovery	End-recovery
rBF (%)	100.00 ± 0.00	216.00 ± 30.30^a	118.80 ± 8.20^b	157.00 ± 20.90^a
BF (ml/100 ml/min)	0.88 ± 0.11	1.84 ± 0.30^a	1.09 ± 0.19^b	1.50 ± 0.34^c
SGVP BF (ml/100 ml/min)	1.13 ± 0.20	5.13 ± 0.32^a	n/a	n/a
Relative change of VO$_2$ (%)	100.00 ± 0.00	324.40 ± 41.50^a	$158.30 \pm 16.60^{a,b}$	$143.60 \pm 16.50^{a,b}$
VO$_2$ (ml O$_2$/100 g/min)	0.05 ± 0.01	0.17 ± 0.04^a	$0.09 \pm 0.03^{a,b}$	$0.08 \pm 0.02^{a,b}$
StO$_2$ (%)	72.70 ± 1.00	57.80 ± 3.10^a	$64.10 \pm 3.00^{a,b}$	$74.50 \pm 0.80^{b,c}$
MAP (mm Hg)	78.50 ± 9.40	92.00 ± 11.00^a	$84.30 \pm 10.0^{a,b}$	$84.10 \pm 9.90^{a,b}$
HR (BPM)	64.70 ± 2.10	82.40 ± 2.70^a	$72.20 \pm 1.60^{a,b}$	$61.90 \pm 3.40^{b,c}$

Blood flow data represent both local [relative changes in blood flow (rBF)/BF] and strain gauge (SGVP BF). All data are reported as means ± standard errors. For MAP, subject 1 is excluded because of poor data quality. Friedman's tests suggest that the effects of time periods are significant for all the parameters measured.
n/a represents not applicable.
[a]Statistically significant difference ($p < 0.05$) from baseline values as determined by Wilcoxon signed-rank test.
[b]Significant difference from end-exercise values.
[c]Significant difference from 1-min recovery values.

metabolic parameters throughout recovery suggest a persistent systemic upregulation of tissue hemodynamics and metabolism, which extended far beyond the end of exercise.

4 Discussion and Conclusions

Our recent use of calibration techniques and dynamometer-gating exercise protocols in forearms had not been tailored to the lower limb, nor had we developed a protocol for exercise that would be comparable to literature. We addressed these in this study by developing exercise and calibration protocols for use in the lower limb that were comparable in duration and intensity to other studies and could be done by both healthy controls and PAD patients. After reviewing literature and testing different exercise protocols in both healthy and PAD subjects,[47] we decided to employ 3 min of 0.5 Hz, 30% MVIC, full range of plantar flexion exercise. This protocol allowed us to establish a complete hemodynamic/metabolic profile of typical responses to moderate exercise in lower limb muscles. Furthermore, due to the similarity of this exercise protocol with those of the literature, we could compare our results with others.[5,12,13,18,39]

Secondary to the above motivation was the desire to compare concurrent flow measurements by our optical technique and SGVP. Such investigation marked a unique aspect of our study, as we had not concurrently measured BF with other techniques, but only compared the results of BF calibrations with literature. By concurrently measuring resting BF with both methods during the same VO protocol, we could remove procedural, temporal, and subject population variables from consideration, allowing for accurate comparisons. In addition, HR and MAP were also continuously recorded in this study by a finger plethysmograph sensor throughout the exercise to examine global cardiovascular responses to exercise. Overall, methods employed in this study made this one of the few studies to comprehensively document local muscle BF, global limb BF, muscle blood oxygen saturation, the derived metabolic parameter of muscle oxygen consumption rate, as well as global cardiovascular output, continuously throughout dynamic exercise.

There were also technical challenges to overcome when translating our techniques from the arm to the leg. ATTs on top of calf muscles are generally greater than those on top of forearm muscles. As such, we modified our fiber-optic probe with a larger S-D distance of 2.5 cm for BF measurements. Based on photon diffusion theory, the larger S-D distance enabled deeper penetration of light, allowing for the detection of BF in deep calf muscles. On the other hand, the larger S-D distance led to lower SNR due to weaker light intensity detected. This study used fiber bundles to detect and average DCS signals from multiple detector fibers, which significantly improved the SNR of BF detections. It should be noted that even with relatively large S-D distances, there are always signal contributions from the top layer adipose tissue to the deep muscle.[6] To reduce the partial volume effect from the top layer tissue, however, layer models are needed for simultaneously quantifying tissue properties in different layers,[48–50] which will be the subject of our future work.

With the advancements described above, this study generated the first local gastrocnemius muscle hemodynamic and global cardiovascular profiles of responses to lower limb exercise. Gated and calibrated measurements made by the combined DCS/NIRS hybrid probe allowed for the continuous acquisition of absolute unit measurements of BF, hemoglobin concentrations, blood oxygen saturation, and oxygen consumption rate of exercising muscle.

Baseline calibration values for these quantities are all comparable to the physiological norms found in other studies,[5,9,18,28,40,51] indicating fidelity of our instrumentation and methods for quantifying these parameters. For example, baseline BF values observed by NIRS and SGVP with the VO protocol in this study (0.88 ± 0.4 and 1.13 ± 0.6 ml/100 ml/min) fell in the range of 0.7 to 4.0 ml/100 ml tissue/min, reported in the literature.[4,5,13,21,51–53] The large variations observed in different studies may be due to the differences in populations and methodologies (i.e., NIRS,[4,51,53] Doppler ultrasound,[13,21] Xe-clearance,[52] SGVP[5]). Similarly, baseline $\dot{V}O_2$ values quantified

by NIRS with AO protocol (0.05 ± 0.03 ml $O_2/100$ g/min) are comparable with the reported values of 0.05 ± 0.01 ml $O_2/100$ g/min in a study of forearm muscles.[41] These consistent findings with the literature and the observed correlation between optical and SGVP resting baseline flows suggest that our calibration procedures are sound. These results support the calibrations of optical spectroscopies using VO and AO to obtain absolute baseline values of muscle hemodynamics and metabolism.

Continuous hemodynamic profiles during exercise demonstrate a moderate challenge to the muscle tissue. Despite the variations in individual subject responses to exercise, there are clear tendencies during exercise for rapid increases in rBF and r$\dot{V}O_2$ along with rapid decreases of THC and StO_2 at the beginning of exercise, which meet the expectation of muscle physiological responses to exercise. After a sharp decrease at the beginning of exercise, THC starts increasing gradually toward the baseline level due to the increase in BF during exercise. During the recovery period, THC stabilizes at a level higher than its pre-exercise baseline, which is also consistent with the elevated BF postexercise. These dynamic changes in muscle oxygenation throughout the exercise protocol agree with dynamic trends measured by NIRS in another study using a similar exercise protocol.[6] Due to the lack of techniques for continuous monitoring of muscle hemodynamic responses during exercise, it is difficult to find literature for comparison. Instead, we compare hemodynamic responses immediately postexercise (i.e., 1-min recovery) with those studies using similar exercise protocols. Postexercise elevation in muscle hemodynamics is observed to be characteristic for all subjects measured in this study and has been noted by many other studies.[5,6,12,18,35] The 1-min recovery rBF values ($118.80 \pm 8.20\%$) observed in this study agree with that of 108% (83% to 139%) measured by DCS immediately postplantar flexion exercise.[12] In addition, the relative increases in SGVP signals measured immediately postexercise (1.13 ± 0.20 ml/100 ml/min at baseline to 5.13 ± 0.32 ml/100 ml/min immediately after exercise) agree well with the reported approximately fivefold increases of SGVP signals postexercise in a study using a similar exercise protocol.[5] StO_2 responses ($64.10 \pm 3.00\%\%$) immediately postexercise also fall in the range of 50% to 65%, observed in other studies using similar exercise protocols.[6,12] r$\dot{V}O_2$ values ($158.30 \pm 16.60\%$) immediately postexercise also agree with a ~160% increase after a walking test, measured by NIRS with AO protocol.[18]

BF in the recovery period is generally elevated compared to baseline, suggesting that exercise has a long-lasting effect on BF. The same trend was also reported in another study where BF increased from slightly over 100% immediately after exercise toward 150% at 3 min postexercise.[12] Few studies measure long recovery times, and we did not measure long enough to observe a complete return to the baseline for most parameters; thus, the actual extent of upregulation merits further investigation. Nevertheless, the local hemodynamic upregulation along with the persistent MAP increase observed in this study indicate that even short duration challenging exercises can induce potent and long-lived physiological effects.[9,12]

The gating algorithm during exercise is necessary due to the sensitivity of DCS to muscle fiber motion. The effect of motion artifacts on ungated DCS data is very potent, and its extent is noted in previous publications from our lab and other groups using different speckle correlation techniques.[6,9,12,32]

The removal of these artifacts via gating means that DCS can produce rapid, continuous examination of microvascular muscle BF during exercise, which is a unique functionality of the system. The loss of flow measurement during the contraction itself is not a major concern since it is widely agreed that microvascular BF can nearly cease during strong muscle contractions due to the high intramuscular pressures generated.[54–56]

It was noted that exercise variations in strain gauges could be quite wide with large errors that may lead to a loss of correlation between the local muscle and global limb flow measurements.[57] Many concerns have arisen over the viability of using SGVP to measure BF during or following dynamic exercise protocols.[41,58] SGVP measures the change in limb circumference and thereby calculates the rate of the change during VO as inflowing blood. SGVP assumes that circumference change is caused by BF. However, it is well documented that dynamic measurements using a strain gauge can be greatly affected by fluid shifts typical of working or exercising limbs (e.g., bone flow, interstitial fluids).[21,58] Such concerns are demonstrated clearly in this study by the large elevation of flow recorded by the strain gauge after the halt of exercise despite rapid local recovery of rBF, r$\dot{V}O_2$, THC, and StO_2 measured by DCS/NIRS. Also, the VO protocol with SGVP measurement cannot be done continuously during exercise. By contrast, our DCS measures microvascular BF in the local muscle directly and continuously throughout exercise (with our gating algorithm) without the need of VO. As such, local muscle BF measured by DCS and whole limb flow measured by SGVP are not expected to have a strictly linear relationship, although SGVP can still be used as the comparison of resting flow with the calibrated DCS. Taken together, we believe that DCS is more reliable than SGVP for continuous monitoring of microvascular BF in local exercising muscle. Because hemodynamic differences between healthy and diseased (e.g., PAD) muscles are not always apparent at rest, it is essential to quantify continuous hemodynamic profiles of local muscles during exercise for accurate diagnoses.[12]

In conclusion, we have successfully vetted our optical calibrations and translated our unique methods from the forearm to the lower limb, as well as developed an exercise measurement regime that can be applied to measure dynamic lower limb exercise free of motion artifacts. The protocol design and exercise response in global and local metabolism observed in this study are comparable to studies using similar protocols. The combination of noninvasiveness, locality, and rapid continuous acquisition of data with the broad coverage of hemodynamic and metabolic parameters allows for a precise physiological profiling of skeletal muscle during dynamic exercises. Results from this study have built the foundation of typical healthy control exercise hemodynamic profiles to which future diseased subject profiles may be compared.

Acknowledgments

References

1. J. D. Briers, "Laser Doppler, speckle and related techniques for blood perfusion mapping and imaging," *Physiol. Meas.* **22**(4), R35–66 (2001).

2. F. Harel et al., "Near-infrared spectroscopy to monitor peripheral blood flow perfusion," *J. Clin. Monit. Comput.* **22**(1), 37–43 (2008).

3. H. Liu et al., "Noninvasive investigation of blood oxygenation dynamics of tumors by near-infrared spectroscopy," *Appl. Opt.* **39**(28), 5231–5243 (2000).

4. M. C. Van Beekvelt et al., "Performance of near-infrared spectroscopy in measuring local O_2 consumption and blood flow in skeletal muscle," *J. Appl. Physiol.* **90**(2), 511–519 (2001).

5. T. A. Bauer et al., "Skeletal muscle StO_2 kinetics are slowed during low work rate calf exercise in peripheral arterial disease," *Eur. J. Appl. Physiol.* **100**(2), 143–151 (2007).

6. G. Yu et al., "Time-dependent blood flow and oxygenation in human skeletal muscles measured with noninvasive near-infrared diffuse optical spectroscopies," *J. Biomed. Opt.* **10**(2), 024027 (2005).

7. R. R. Wolfe, "The underappreciated role of muscle in health and disease," *Am. J. Clin. Nutr.* **84**(3), 475–482 (2006).

8. M. Ferrari, M. Muthalib, and V. Quaresima, "The use of near-infrared spectroscopy in understanding skeletal muscle physiology: recent developments," *Philos. Trans. R. Soc. A: Math., Phys. Eng. Sci.* **369**(1955), 4577–4590 (2011).

9. K. Gurley, Y. Shang, and G. Yu, "Noninvasive optical quantification of absolute blood flow, blood oxygenation, and oxygen consumption rate in exercising skeletal muscle," *J. Biomed. Opt.* **17**(7), 075010 (2012).

10. T. Binzoni et al., "Energy metabolism and interstitial fluid displacement in human gastrocnemius during short ischemic cycles," *J. Appl. Physiol.* **85**(4), 1244–1251 (1998).

11. M. P. Francescato, V. Cettolo, and P. E. Di Prampero, "Relationships between mechanical power, O_2 consumption, O_2 deficit and high-energy phosphates during calf exercise in humans," *Pflugers Arch—Eur. J. Physiol.* **445**(5), 622–628 (2003).

12. R. C. Mesquita et al., "Diffuse optical characterization of an exercising patient group with peripheral artery disease," *J. Biomed. Opt.* **18**(5), 057007 (2013).

13. V. Quaresima et al., "Calf and shin muscle oxygenation patterns and femoral artery blood flow during dynamic plantar flexion exercise in humans," *Eur. J. Appl. Physiol.* **84**(5), 387–394 (2001).

14. M. Saito, T. Mano, and S. Iwase, "Changes in muscle sympathetic nerve activity and calf blood flow during static handgrip exercise," *Eur. J. Appl. Physiol.* **60**(4), 277–281 (1990).

15. W. G. Schrage et al., "Roles of nitric oxide synthase and cyclooxygenase in leg vasodilation and oxygen consumption during prolonged low-intensity exercise in untrained humans," *J. Appl. Physiol.* **109**(3), 768–777 (2010).

16. B. E. Van Leeuwen et al., "Calf blood flow and posture: Doppler ultrasound measurements during and after exercise," *J. Appl. Physiol.* **72**(5), 1675–1680 (1992).

17. D. H. Wiener et al., "Abnormal skeletal muscle bioenergetics during exercise in patients with heart failure: role of reduced muscle blood flow," *Circulation* **73**(6), 1127–1136 (1986).

18. H. M. Kooijman et al., "Near infrared spectroscopy for noninvasive assessment of claudication," *J. Surg. Res.* **72**(1), 1–7 (1997).

19. C. Askew, "Exercise intolerance in peripheral arterial disease," PhD Thesis, Queensland University of Technology, Brisbane, Australia (2002).

20. E. Selvin and T. P. Erlinger, "Prevalence of and risk factors for peripheral arterial disease in the United States: results from the National Health and Nutrition Examination Survey, 1999–2000," *Circulation* **110**(6), 738–743 (2004).

21. G. Radegran, "Limb and skeletal muscle blood flow measurements at rest and during exercise in human subjects," *Proc. Nutr. Soc.* **58**(4), 887–898 (1999).

22. T. Durduran, "Non-invasive measurements of tissue hemodynamics with hybrid diffuse optical methods," PhD Thesis, University of Pennsylvania (2004).

23. M. P. Francescato and V. Cettolo, "Two-pedal ergometer for in vivo MRS studies of human calf muscles," *Magn. Reson. Med.* **46**(5), 1000–1005 (2001).

24. O. U. Scremin et al., "Preamputation evaluation of lower-limb skeletal muscle perfusion with H(2) (15)O positron emission tomography," *Am. J. Phys. Med. Rehabil.* **89**(6), 473–486 (2010).

25. G. Yu et al., "Validation of diffuse correlation spectroscopy for muscle blood flow with concurrent arterial spin labeled perfusion MRI," *Opt. Express* **15**(3), 1064–1075 (2007).

26. R. Boushel et al., "Regional blood flow during exercise in humans measured by near-infrared spectroscopy and indocyanine green," *J. Appl. Physiol.* **89**(5), 1868–1878 (2000).

27. S. J. Matcher and C. E. Cooper, "Absolute quantification of deoxyhaemoglobin concentration in tissue near infrared spectroscopy," *Phys. Med. Biol.* **39**(8), 1295–1312 (1994).

28. L. A. Paunescu et al., "Calf muscle blood flow and oxygen consumption measured with near-infrared spectroscopy during venous occlusion," *Proc. SPIE* **3597**, 317 (1999).

29. D. M. Hueber et al., "New optical probe designs for absolute (self-calibrating) NIR tissue hemoglobin measurements," *Proc. SPIE* **3597**, 618 (1999).

30. S. Fantini et al., "Frequency-domain multichannel optical detector for noninvasive tissue spectroscopy and oximetry," *Opt. Eng.* **34**(1), 32–42 (1995).

31. D. A. Boas, "Diffuse photon probes of structural and dynamical properties of turbid media: theory and biomedical applications," PhD Thesis, University of Pennsylvania (1994).

32. Y. Shang et al., "Effects of muscle fiber motion on diffuse correlation spectroscopy blood flow measurements during exercise," *Biomed. Opt. Express* **1**(2), 500–511 (2010).

33. M. N. Kim et al., "Noninvasive measurement of cerebral blood flow and blood oxygenation using near-infrared and diffuse correlation spectroscopies in critically brain-injured adults," *Neurocrit. Care* **12**(2), 173–180 (2010).

34. R. C. Mesquita et al., "Direct measurement of tissue blood flow and metabolism with diffuse optics," *Philos. Trans. R. Soc. A: Math., Phys. Eng. Sci.* **369**(1955), 4390–4406 (2011).

35. Y. Shang et al., "Noninvasive optical characterization of muscle blood flow, oxygenation, and metabolism in women with fibromyalgia," *Arthritis Res. Ther.* **14**(6), R236 (2012).

36. Y. Shang et al., "Portable optical tissue flow oximeter based on diffuse correlation spectroscopy," *Opt. Lett.* **34**(22), 3556–3558 (2009).

37. A. D. Edwards et al., "Measurement of hemoglobin flow and blood flow by near-infrared spectroscopy," *J. Appl. Physiol.* **75**(4), 1884–1889 (1993).

38. R. A. De Blasi et al., "Noninvasive measurement of forearm blood flow and oxygen consumption by near-infrared spectroscopy," *J. Appl. Physiol.* **76**(3), 1388–1393 (1994).

39. M. C. Van Beekvelt et al., "Blood flow and muscle oxygen uptake at the onset and end of moderate and heavy dynamic forearm exercise," *Am. J. Physiol. Regul. Integr. Comp. Physiol.* **280**(6), R1741–R1747 (2001).

40. C. Casavola et al., "Blood flow and oxygen consumption with near-infrared spectroscopy and venous occlusion: spatial maps and the effect of time and pressure of inflation," *J. Biomed. Opt.* **5**(3), 269–276 (2000).

41. R. A. De Blasi et al., "Noninvasive measurement of human forearm oxygen consumption by near infrared spectroscopy," *Eur. J. Appl. Physiol.* **67**(1), 20–25 (1993).

42. H. N. Mayrovitz, "Compression-induced pulsatile blood flow changes in human legs," *Clin. Physiol.* **18**(2), 117–124 (1998).

43. G. Mosti and H. Partsch, "Inelastic bandages maintain their hemodynamic effectiveness over time despite significant pressure loss," *J. Vasc. Surg.* **52**(4), 925–931 (2010).

44. P. S. van Bemmelen et al., "Augmentation of blood flow in limbs with occlusive arterial disease by intermittent calf compression," *J. Vasc. Surg.* **19**(6), 1052–1058 (1994).

45. K. Gurley, "Use of hybrid diffuse optical spectroscopies in continuous monitoring of blood flow, blood oxygenation, and oxygen consumption rate in exercising skeletal muscle," MS Thesis, University of Kentucky (2012).

46. T. Durduran et al., "Diffuse optics for tissue monitoring and tomography," *Rep. Prog. Phys.* **73**(7), 076701 (2010).

47. B. Henry, "Stabilization of extended diffuse optical spectroscopy measurements on in vivo human skeletal muscle during dynamic exercise," MS Thesis, University of Kentucky (2014).

48. Y. Shang et al., "Extraction of diffuse correlation spectroscopy flow index by integration of Nth-order linear model with Monte Carlo simulation," *Appl. Phys. Lett.* **104**(19), 193703 (2014).

49. Y. Shang and G. Yu, "A Nth-order linear algorithm for extracting diffuse correlation spectroscopy blood flow indices in heterogeneous tissues," *Appl. Phys. Lett.* **105**(13), 133702 (2014).

50. T. Li et al., "Simultaneous measurement of deep tissue blood flow and oxygenation using noncontact diffuse correlation spectroscopy flow-oximeter," *Sci. Rep.* **3**, 1358 (2013).

51. S. Fantini et al., "Spatial mapping of blood flow and oxygen consumption in the human calf muscle using near-infrared spectroscopy," *Proc. SPIE* **4241**, 69 (2001).

52. R. Boushel et al., "Blood flow and oxygenation in peritendinous tissue and calf muscle during dynamic exercise in humans," *J. Physiol.* **524**(1), 305–313 (2000).

53. S. Nioka et al., "A novel method to measure regional muscle blood flow continuously using NIRS kinetics information," *Dyn. Med.* **5**, 5 (2006).

54. D. Richardson, "Blood flow response of human calf muscles to static contractions at various percentages of MVC," *J. Appl. Physiol.* **51**(4), 929–933 (1981).

55. R. J. Korthuis, "Skeletal muscle blood flow is pulsatile during rhythmic exercise," in *Skeletal Muscle Circulation*, R. J. Korthuis, Ed., p. 38, Morgan and Claypool Life Sciences, San Rafael, California (2011).

56. J. E. Hall, "Muscle blood flow and cardiac output during exercise; the coronary circulation and ischemic heart disease," Chapter 21 in *Guyton and Hall Textbook of Medical Physiology*, J. E. Hall, Ed., pp. 243–246, Elsevier, St. Louis, Missouri (2011).

57. R. J. Whitney, "The measurement of volume changes in human limbs," *J. Physiol.* **121**(1), 1–27 (1953).

58. W. R. Hiatt et al., "Venous occlusion plethysmography reduces arterial diameter and flow velocity," *J. Appl. Physiol.* **66**(5), 2239–2244 (1989).

Brad Henry has recently graduated from the Department of Biomedical Engineering at the University of Kentucky. He has been working on the development and application of hybrid near-infrared spectroscopy and diffuse correlation spectroscopy for noninvasive assessment of tissue blood flow, blood oxygenation, and metabolic rate of oxygen consumption in exercising skeletal muscles.

Mingjun Zhao is a graduate student in the Department of Biomedical Engineering at the University of Kentucky. She has been working on the development of diffuse correlation spectroscopy and tomography for noninvasive assessment and imaging of blood flow distributions in animal and human tissues, including skeletal muscles.

Yu Shang received his PhD in biomedical engineering in 2008. He was a research scientist working in the Department of Biomedical Engineering at the University of Kentucky and is now working as a faculty member in the Department of Biomedical Engineering at the North University of China. His current research interests focus on the development of near-infrared diffuse optical spectroscopy and diffuse correlation spectroscopy for noninvasive assessment of microvasculature blood flow/oxygenation/oxygen metabolism in biological tissues.

Timothy Uhl is a professor in the Department of Rehabilitation Science at the College of Health Sciences, University of Kentucky, and director of the Musculoskeletal Laboratory. His research interests include upper extremity musculoskeletal injuries, clinical interventions of rehabilitation protocols for upper and lower extremities, and musculoskeletal functional assessment used for return to work or sport.

D. Travis Thomas is an assistant professor at the College of Health Sciences, University of Kentucky. He has extensive experience with clinical exercise trials involving diet modification and assessment, database management, and body composition analysis. His work focuses on vitamin D and other nutritional interventions for improving health in the overweight, aging, and those with cancer.

Eleftherios S. Xenos is an associate professor of vascular surgery at the University of Kentucky and chief of the Vascular Surgery Section at the VA Medical Center in Lexington, Kentucky. He has specific clinical training and expertise in vascular surgery as well as clinical research experience in the studies of cerebral vascular disease, aortic aneurysm disease, and peripheral artery disease.

Sibu P. Saha is a professor of surgery at the College of Medicine, University of Kentucky. He has been in the practice of vascular surgery for over 30 years. He currently serves as a chief at the Division of Cardiothoracic Surgery and a chairman at the UK Directors Council Gill Heart Institute. He has actively worked on several clinical studies of cerebral vascular disease using diffuse optical technologies.

Guoqiang Yu is an associate professor of the Department of Biomedical Engineering at the University of Kentucky. He has over 20 years of experience in the field of biomedical engineering and is currently leading a research group to develop various near-infrared diffuse spectroscopy and tomography systems for noninvasive imaging of deep tissue hemodynamics in animals and humans.